Surface and Interfacial FTIR Spectroscopic Studies of Latexes. XIII. Surfactant Exudation in Silicone-Modified Latex Films

B.-J. NIU and MAREK W. URBAN*

Department of Polymers and Coatings, North Dakota State University, Fargo, North Dakota 58105

SYNOPSIS

Exudation of sodium dioctylsulfosuccinate (SDOSS) surfactant molecules to the film–substrate (F–S) and film–air (F–A) interfaces in styrene/*n*-butyl acrylate (Sty/*n*-BA) latex films in the presence of trimethoxysilyl propylmethacrylate (MSMA) molecules was examined by polarized attenuated total reflection Fourier transform infrared (ATR FTIR) spectroscopy. It appears that SDOSS molecules are present at the F–A interface but are not detected at the F–S interface due to their displacement by MSMA. When the second layer of latex is deposited on the previously coalesced latex film with the same composition, SDOSS molecules are detected at the F–A of the top overlayer and the interfacial regions between both films. While the top film contains SDOSS surfactant molecules in their free or COOH hydrogen-bonded forms, the interfacial regions between the films exhibit arrays of SDOSS molecules preferentially parallel to the film surface. © 1996 John Wiley & Sons, Inc.

INTRODUCTION

Silicone-containing coatings are known for their outstanding thermal and photolytic stabilities. In general, their heat and weather resistance are closely related to the amount of silicone content in a given polymer network.[1] Furthermore, silanes added to a coating formulation are known to improve numerous properties. For that reason, silanes in their hydrolyzed form added to latex suspensions may result in a coalesced polymer network with significantly altered properties. If one believes that interpenetrating networks (IPN) exist, the term IPN would be used to describe polymers in which silane sub-networks are interpenetrated by entanglements of high-molecular-weight copolymers. However, when such silanes are added to an aqueous suspension, reactions of these species in the latex aqueous suspensions usually involves hydrolysis of siloxane groups, leading to the silanol formation, followed by silanol condensation which may occur on surfaces of latex particles. Finally, if the surface reactions are favorable, a crosslinked polymer network is formed after coalescence.[2] Figure 1 illustrates schematically how silanes may become incorporated into a latex network.

With these considerations in mind, let us recall our previous studies[3-11] which were concerned with the exudation of sodium dioctylsulfosuccinate (SDOSS) surfactant molecules in latex films. These studies indicated that there is a significant influence of interfaces on mobility of small molecules in latex films.[9] As a result, various properties, including adhesion, durability, and thermal resistance, may be affected. Since the presence of silanes may inherently alter already attractive properties of latexes, this issue stimulated us to expand the scope of our research program, and examine the behavior of SDOSS in styrene/*n*-butylacrylate (Sty/*n*-BA) latexes containing silanes. We have chosen trimethoxysilyl propylmethacrylate with the formula $H_2CCCH_3COOCH_2CH_2CH_2Si(OCH_3)_3$(MSMA). As in our previous studies, polarized attenuated total reflection Fourier transform infrared (ATR FTIR) spectroscopy, along with the recently developed algorithm,[4,5] will be utilized to monitor SDOSS and MSMA molecules at the film–air (F–A) and film–

* To whom correspondence should be addressed.

Journal of Applied Polymer Science, Vol. 60, 389–397 (1996)
 CCC 0021-8995/96/030389-09

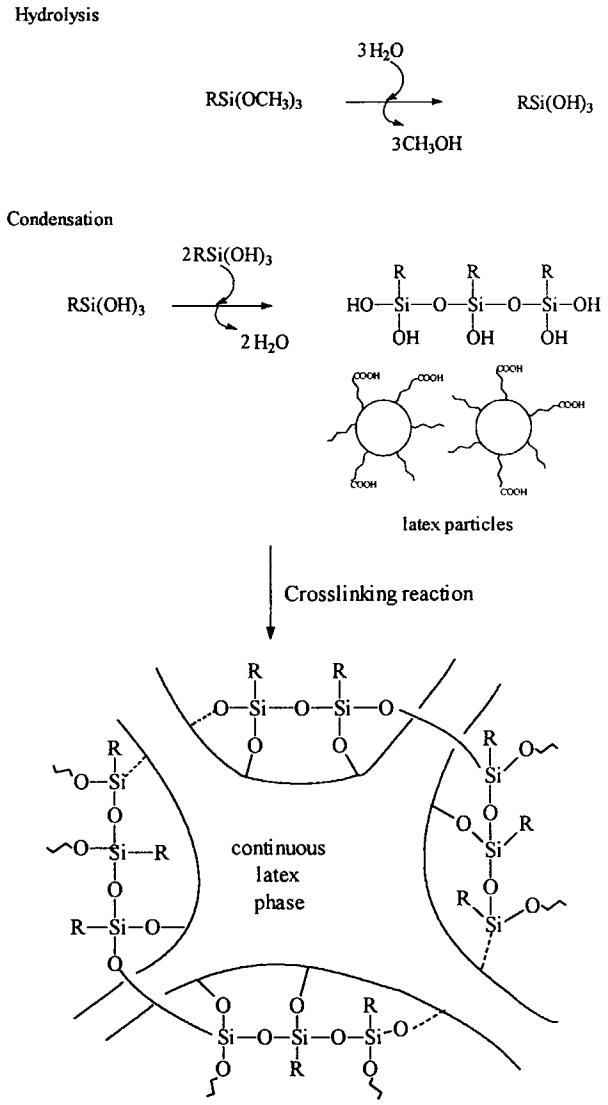

Figure 1 Schematic diagram of reaction mechanism for silicone modifiers during latex coalescence.

substrate (F–S) interfaces. In this contest, we are particularly interested in the mobility and diffusion of SDOSS and MSMA molecules near the F–A and F–S interfaces.

EXPERIMENTAL

Preparation of Silicone-Modified Latexes

50%/50% Sty/*n*-BA copolymer latex was synthesized by semicontinuous emulsion polymerization, as described in our previous publications.[3] MSMA was neutralized with 1 N NaOH aqueous solution to achieve approximate basicity (pH = 8), promoting hydrolysis of MSMA. This solubilized 10% w/w hydrolyzed MSMA monomer was slowly added to the latex solution while stirring. Typically, 6 h were allowed for MSMA hydrolysis and silanol formation. Thus prepared, silicone-modified latex aqueous dispersion was cast on polytetrafluoroethylene (PTFE) substrate, and allowed to coalesce for 72 h under ambient conditions. All films were approximately 200 μm thick.

Spectroscopic Measurements

ATR FTIR spectroscopy was utilized to monitor the mobility of surfactant and MSMA molecules at the both F–A and F–S interfaces. ATR FTIR spectra were collected on a Digilab FTS-20 instrument equipped with an ATR cell (Spectra Tech) equipped with a KRS-5 crystal. In a typical experiment, 200 scans were collected at a resolution of 4 cm^{-1} with a transverse electric (TE) (90°) polarizer filter. The rectangular ATR attachment (Spectra Tech) was equipped with a KRS-5 crystal aligned to give a series of incident beam angles from 40 to 60 degrees. All spectra were transferred to an PC-compatible computer for further spectral analysis utilizing Spectra Calc software (Galactic, Inc.). The spectra were corrected for optical effects using the Q-ATR algorithm.[4,5]

RESULTS AND DISCUSSION

In the previous studies,[6–15] we focused on the C—O and S—O stretching regions of SDOSS surfactant molecules because analysis of the band intensities resulting from hydrophobic and hydrophilic entities of SDOSS allowed us not only the detection of surfactant molecules near the F–A and F–S interfaces, but also elucidation of their orientation. These studies also indicated that the presence of surfactant molecules at the interfaces may have a significant effect on film properties. In an effort to control the surfactant mobility and simultaneously control latex film properties, MSMA can be incorporated into a latex formulation. While the Experimental section provides necessary details regarding latex synthesis and film preparation, here we shall address how the presence of MSMA may affect, if at all, the distribution and mobility of surfactant molecules in 50%/50% Sty/*n*-BA latexes.

As a first step in the analysis, let us establish spectral features resulting from the presence of MSMA in Sty/*n*-BA latex. Figure 2 illustrates a series of ATR FTIR spectra recorded from the F–S interfaces of the latex films composed of 100%

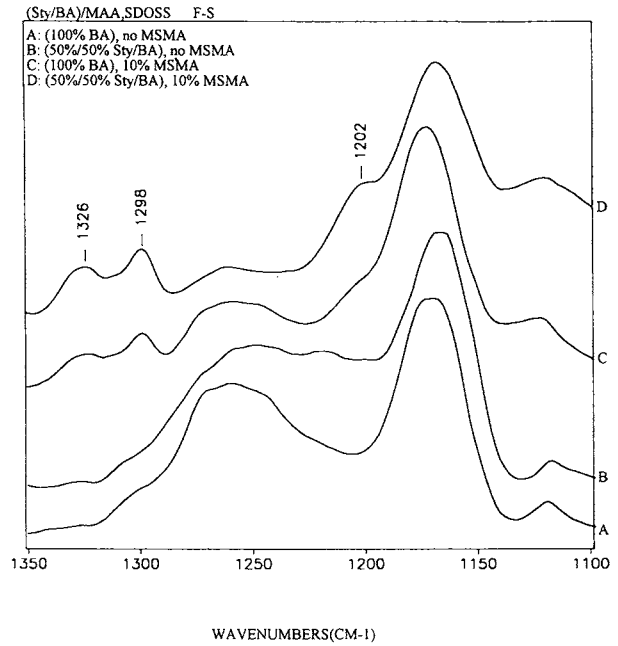

Figure 2 ATR FTIR spectra of various Sty/*n*-BA latex copolymers with and without MSMA in S—O asymmetric stretching vibrational modes at F–S interface: (A) 100% *n*-BA without MSMA; (B) 50/50% Sty/*n*-BA without MSMA; (C) 100% *n*-BA with MSMA; (D) 50/50% Sty/*n*-BA with MSMA.

poly(*n*-BA) and 50%/50% Sty/*n*-BA. This choice of composition was dictated by the compatibility differences between Sty and *n*-BA components with respect to SDOSS, and the glass transition temperatures (T_gs) of latex polymers. Traces (A) and (C) of Figure 2 illustrate the spectra of 100% *n*-BA without and with MSMA, respectively. It is apparent that the bands at 1326, 1298, and 1202 cm^{-1} are detected when the latex contains MSMA. These bands are attributed to the in-plane $H_2C{=}C$ deformation (1326 and 1298 cm^{-1}) and $Si{-}CH_2$ symmetric stretching (1202 cm^{-1}) modes of MSMA. When the latex T_g is increased by changing its composition to 50%/50% Sty/*n*-BA, the bands due to MSMA become more pronounced, indicating that a higher content of MSMA is detected near the F–S interface. This is demonstrated by the presence of significantly stronger MSMA bands at 1326, 1298, and 1202 cm^{-1} [trace (D), Figure 2].

Temporarily postponing evaluation of how latex composition may affect the distribution of MSMA, let us consider Figure 3, which shows ATR FTIR spectra of the same specimens but in the S—O stretching region. As we recall, our previous studies[3,6-14] indicated that there are two bands, at 1046 and 1056 cm^{-1}, which are attributed to the S—O bands resulting from H-bonding associations of the S—O bonds with H_2O molecules and COOH groups on the latex surface, respectively. A comparison of traces (A) and (C) of Figure 3 indicates that when MSMA is added to 100% *n*-BA latex formulation, the 1056 and 1046 cm^{-1} bands are not detected. Interestingly, the band at 1056 cm^{-1} is not detected at all, regardless of the presence of MSMA.

In view of the above observations, let us first consider the absence of the 1046 cm^{-1} band in the spectra of a specimen containing MSMA. Since this band results from the $SO_3^-Na^+$ and H_2O interactions, the presence of MSMA causes the displacement of SDOSS molecules from the F–S interface. In order to identify the origin of this phenomenon, let us recall that the presence of the 1056 cm^{-1} band was found to be a function of two factors: a particle size and a latex particle composition.[15] As we recall our previous studies[15] conducted on 50%/50% Sty/*n*-BA latexes with the particle sizes of 50 and 100 nm, the 1056 cm^{-1} was detected only for latexes with 100-nm particles. In this study, we also used a 50-nm-particle latex, in which the 1056 cm^{-1} was not detected.

In an effort to understand how particle size would alter $SO_3^-Na^+ \cdots HOOC$ interactions, let us realize that a larger latex particle size is accomplished by

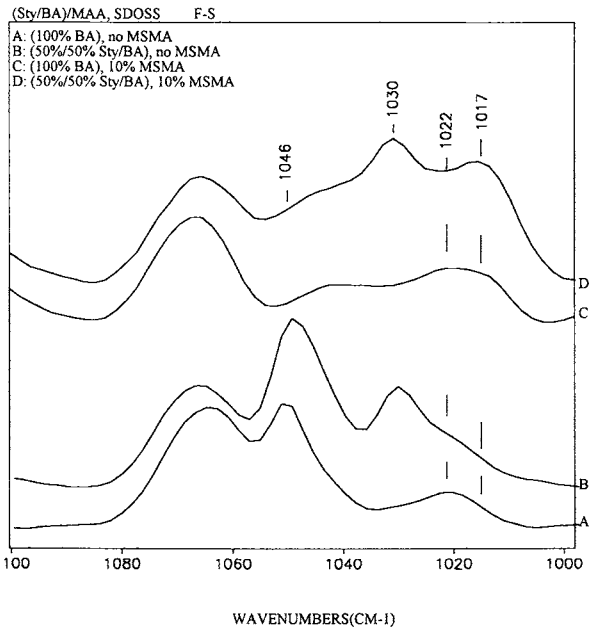

Figure 3 ATR FTIR spectra of various Sty/*n*-BA latex copolymers with and without MSMA in S—O symmetric stretching vibrational modes at F–S interface: (A) 100% *n*-BA without MSMA; (B) 50/50% Sty/*n*-BA without MSMA; (C) 100% *n*-BA with MSMA; (D) 50/50% Sty/*n*-BA with MSMA.

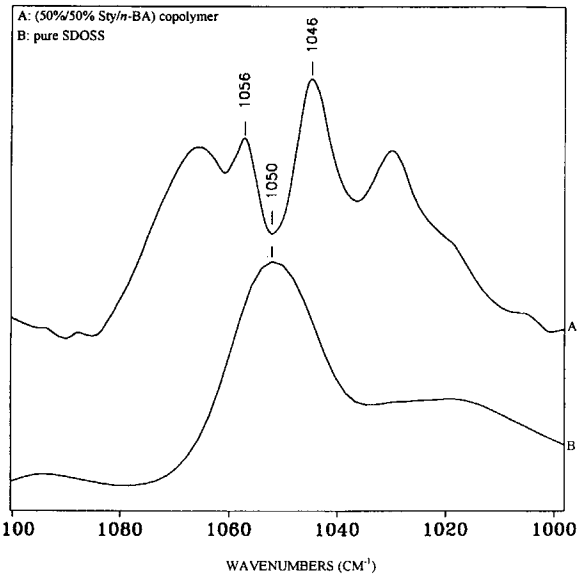

Figure 4 ATR FTIR spectra: (A) 50%/50% Sty/n-BA copolymer with a particle size of 100 nm; (B) pure SDOSS surfactant molecules.

slower stirring of the reaction mixture during latex polymerization. Under such circumstances, the reactivity ratio of the starting monomers will have a major influence on a latex particle composition. As we established in our previous studies and discussed in the context of the reactivity ratios for Sty and n-BA published in the literature,[14] the reactivity ratios of styrene and n-BA favor homopolymerization of styrene. As a result, preferential formation of polystyrene core and poly(n-BA) shell is anticipated. If this is the case, a sufficient amount of COOH groups is available for interactions with hydrophilic ends of SDOSS, and the 1056 cm^{-1} band is detected.

A smaller particle size can be achieved by a vigorous stirring of polymerizing suspension, which subsequently will diminish the influence of reactivity ratios during latex polymerization, thus enhancing the probability of random copolymerization. Therefore, using the same composition of starting materials, smaller particles with more uniform distribution of Sty/n-BA within each particle will be produced. Hence, fewer COOH species will be available for H-bonding with $SO_3^-Na^+$ hydrophilic SDOSS ends. In an effort to further justify that the particle size may affect the presence of acid groups near the surface, a mixture of 50%/50% w/w of poly(Sty) and poly(n-BA) homopolymerized latexes in separate batches was allowed to coalesce. In this case, the band at 1056 cm^{-1} was present [Fig. 4, trace (A)]. In contrast, the ATR spectrum of pure SDOSS shows that only the 1050 cm^{-1} band is detected. This is shown in Figure 4, trace (B). This observation indicates that, for the same particle size homopolymers of polySty and poly(n-BA), there are either islands of poly(n-BA), which allow the $SO_3^-Na^+$ and COOH groups to interact with each other, or there is an excess of poly(n-BA) near the latex film surface, allowing for the same type of interactions. Based on these observations, for a large Sty/n-BA particle size there is a higher n-BA content near the latex surface particle, whereas for a smaller particle size, more uniform distribution is anticipated. Figure 5 illustrates how the effect of particle size may influence the Sty/n-BA distribution after coalescence.

Having identified the effects of particle size and the particle composition on SDOSS$\cdots$HOOC interactions, let us return to the issue of displacement of SDOSS molecules from the interfaces by MSMA. This phenomenon is particularly pronounced for the 50%/50% Sty/n-BA latex copolymer composition in Figure 2, trace (D). In an effort to understand this behavior, it should be realized that the compatibility among latex components and free volume may play a significant role. For example, 50%/50% Sty/n-BA latex exhibits higher T_g, thus it exhibits a lesser amount of the free volume at a given tem-

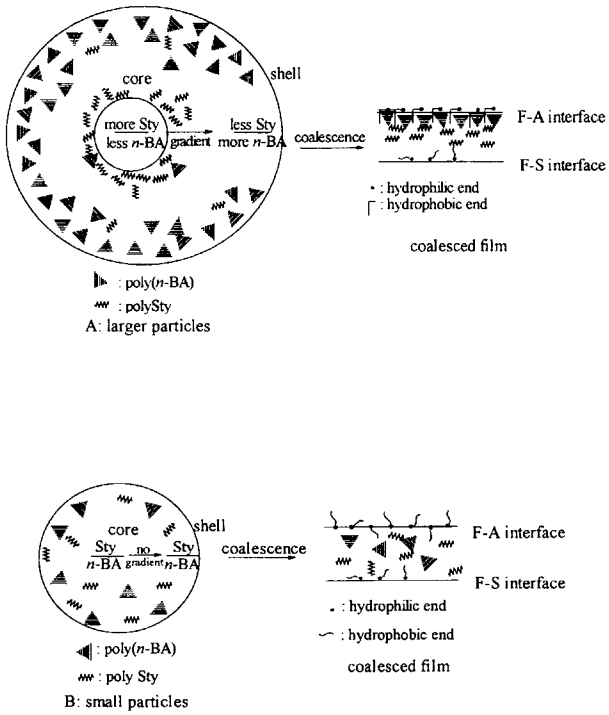

Figure 5 Schematic diagrams of core-shell effect in Sty/n-BA latex copolymers and latex film formation after coalescence: (A) large particle size; (B) small particle size.

perature. Therefore, the ability to diffuse due to the free volume differences and compatibility among the components will play a significant role. For example, poly(n-BA) is more compatible with MSMA than with 50%/50% Sty/n-BA. In view of these considerations, and of the fact that SDOSS is displaced from the F–S interface by MSMA molecules which may form a network between the latex particles, fewer MSMA molecules are available for crosslinking during latex coalescence. As a result, less-pronounced band intensities at 1326, 1298, and 1202 cm^{-1} are detected for 100% n-BA latex [trace (C)]. However, their increase is detected for 50%/50% Sty/n-BA, which is illustrated in Figure 2, traces (C) and (D), respectively, indicating that more MSMA molecules are grafted onto the latex particles in a 50%/50% Sty/n-BA composition.

With this analysis in mind, let us consider the F–A interface. Figure 6 shows a series of ATR FTIR spectra recorded from the F–A interface for 100% n-BA and 50%/50% Sty/n-BA latexes. In essence, these data resemble the data presented in Figure 2, and the only detectable difference is a marginally higher content of MSMA detected for a 50%/50% Sty/n-BA composition. However, as compared to the results for the same specimens at the F–S interface, the S—O stretching region of the F–A interface presented in Figure 7 shows a much weaker S—O stretching band at 1046 cm^{-1} [traces (B) and (D)]. Furthermore, when MSMA is incorporated into the latex formulation it appears that the 1017 cm^{-1} band increases. This is illustrated in traces (C) and (D), Figure 7, and indicates that the Si—OCH_3 groups of MSMA hydrolyze and are able to attach to the latex to form new Si—O—C linkages. This is demonstrated by the presence of the 1017 cm^{-1} band. Recalling the results presented in trace (C) of Figure 2, the band intensities at 1326, 1298, and 1202 cm^{-1} at the F–S interface are stronger than those at the F–A interface [Fig. 6, trace (C)]. Although it is generally accepted that silanes tend to migrate to the F–S interface, which is illustrated in Figure 8(A), molecular level mechanisms responsible for MSMA diffusion are likely attributed to the formation of alkoxy silanes near the surface. After hydrolysis (Fig. 1), methoxy silanes are converted to hydroxyl groups; during coalescence, the covalent bonds between hydroxyl groups on MSMA and latexes are formed near the F–S interface.

If MSMA migrates towards the F–S interface, the film cross-section is not uniform; subsequently, the F–A interface will exhibit an MSMA deficit. Let us now add over the previously coalesced film another layer of the same latex containing the same com-

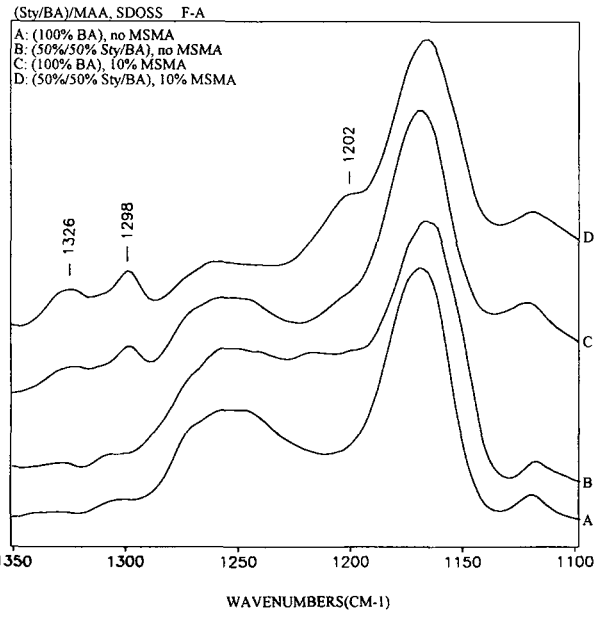

Figure 6 ATR FTIR spectra of various Sty/n-BA latex copolymers with and without MSMA in S—O asymmetric stretching vibrational modes at F–A interface: (A) 100% n-BA without MSMA; (B) 50/50% Sty/n-BA without MSMA; (C) 100% n-BA with MSMA; (D) 50/50% Sty/n-BA with MSMA.

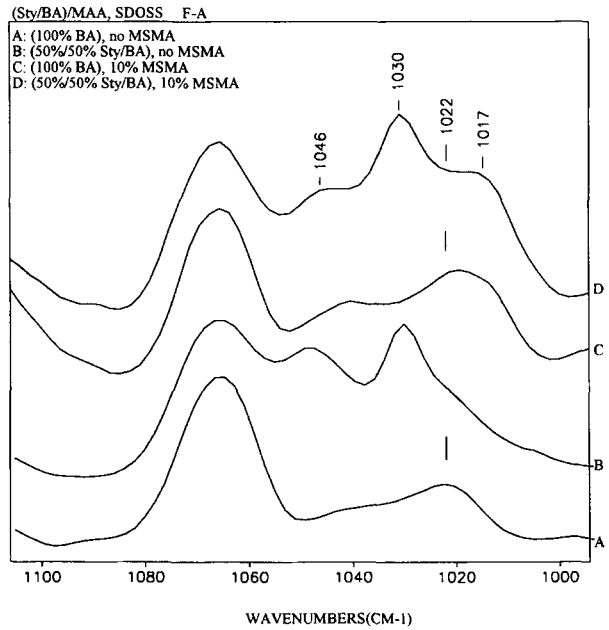

Figure 7 ATR FTIR spectra of various Sty/n-BA latex copolymers with and without MSMA in S—O symmetric stretching vibrational modes at F–A interface: (A) 100% n-BA without MSMA; (B) 50/50% Sty/n-BA without MSMA; (C) 100% n-BA with MSMA; (D) 50/50% Sty/n-BA with MSMA.

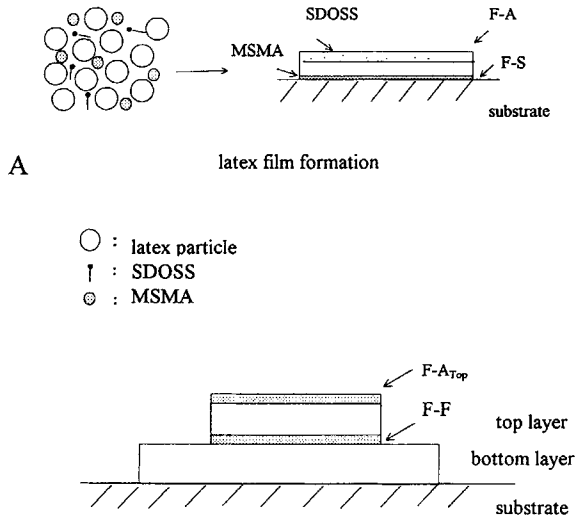

Figure 8 Schematic diagrams of F–A and F–S interfaces in double layer latex film: (A) latex film formation; (B) F–A_{Top} and F–F interfaces at top-layer film.

position of MSMA. When a new latex layer is deposited, the F–A will become the film–film (F–F) interface, and the F–A of the overlayer will become F–A_{Top}. Figure 8(B) defines new F–A_{Top} and F–F interfaces after an approximately 200-μm-thick film of aqueous Sty/*n*-BA was allowed to coalesce over the existing film. Figure 9, traces (A)–(E), show TE-polarized ATR FTIR spectra of 50%/50% Sty/*n*-BA containing 10% MSMA recorded from the F–A_{Top} interface. The ATR spectra were recorded at several angles of incidence, ranging from 40 to 60 degrees. It appears that the 1046 cm^{-1} band is the strongest at 60 degrees [Fig. 9, trace (A)], and its intensity decreases as the angle of incidence becomes smaller. In contrast, the band intensity at 1050 cm^{-1} increases. Following the well-documented fact[16] that the larger the angle of incidence, the shallower the depth of penetration, these observations indicate that the $SO_3^-Na^+$ entities of SDOSS form more associations with the acid latex groups. This is demonstrated by the increasing intensity of the 1046 cm^{-1} band for the shallowest, approximately 1.36-μm, depth, which was obtained with a 60-degree angle of incidence using a KRS-5 crystal. In contrast, the 1050 cm^{-1} band becomes stronger at greater depths, indicating that the SDOSS$\cdots H_2O$ and free SDOSS associations are not as near the surface, as was observed for the SDOSS$\cdots$HOOC— associations. These data also indicate that the acid groups are preferentially near the F–A_{Top} interface and they associate with the SDOSS molecules, resulting in H-bonding. Similar trends are observed in the case of the F–F interface for the top layer, but the magnitude of the changes is much smaller. This is illustrated in Figure 10, traces (A)–(E). Based on the data presented in Figures 9 and 10, it appears that the presence of the MSMA molecules influences the composition of the F–A_{Top} and F–F interfaces. Again, MSMA molecules tend to accumulate near the in-

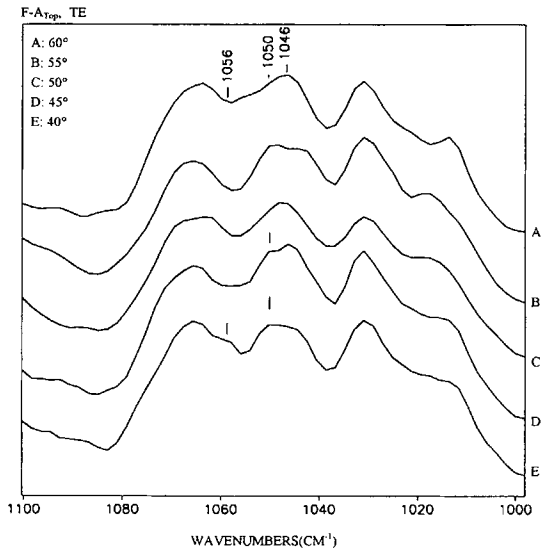

Figure 9 ATR FTIR spectra of S—O symmetric stretching vibrational modes of 50/50% Sty/*n*-BA composition containing 10% MSMA with various incident angles of IR light at F–A interface of top layer with TE polarization: (A) 60°; (B) 55°; (C) 50°; (D) 45°; (E) 40°.

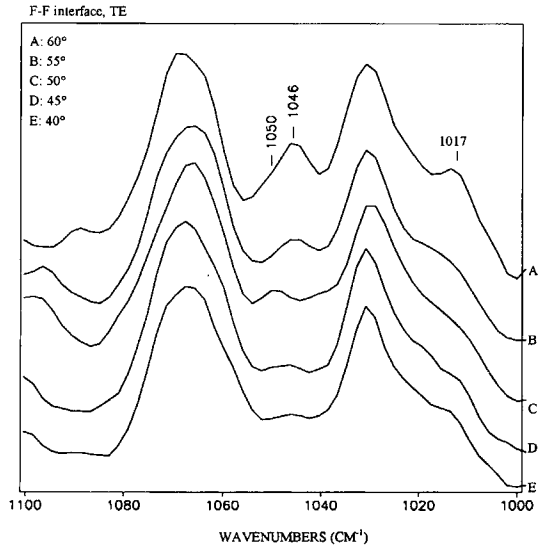

Figure 10 ATR FTIR spectra of S—O symmetric stretching vibrational modes of 50/50% Sty/*n*-BA composition containing 10% MSMA with various incident angles of IR light at F–S interface of top layer with TE polarization: (A) 60°; (B) 55°; (C) 50°; (D) 45°; (E) 40°.

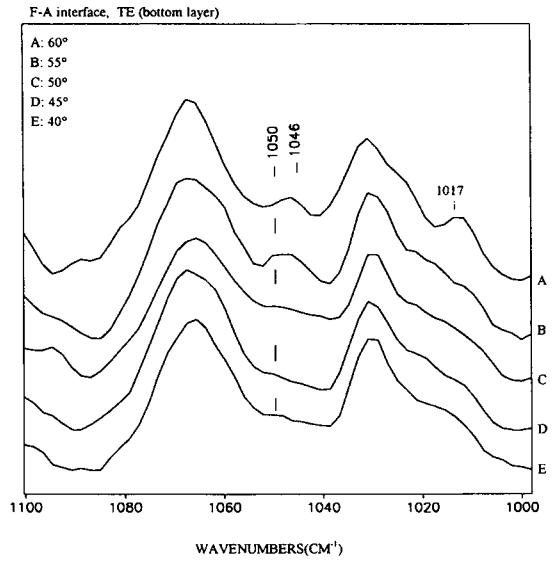

Figure 11 ATR FTIR spectra of S—O symmetric stretching vibrational modes of 50/50% Sty/*n*-BA composition containing 10% MSMA with various incident angles of IR light at F–A interface of bottom layer with TE polarization: (A) 60°; (B) 55°; (C) 50°; (D) 45°; (E) 40°.

terfacial regions of the films, thus displacing SDOSS and allowing them to migrate to the F–A_{Top} interface.

At this point, let us recall the results obtained from the F–A and F–S interfaces without the top layer (Figs. 2 and 3), and cross-examine the same interfaces when the top layer of latex is present. Figure 11 shows ATR FTIR spectra recorded at various incident angles from the F–A interface with TE polarization. The band intensity of the 1046 cm^{-1} band is more pronounced at 60 degrees [trace (A)], indicating that, at approximately 1.36 μm, there are again SDOSS· · ·HOOC— associations. Surprisingly, however, and in contrast to the previous results, the 1050 cm^{-1} band due to free SDOSS molecules appears to be the strongest at 55 degrees. Because this angle of incidence corresponds to approximately 1.49 μm in depth, this observation indicates that there is a double-layer structure near the surface. At the top F–A_{Top}, there are SDOSS· · ·HOOC— associations, and underneath, there are arrays of unassociated SDOSS molecules. Furthermore, near 1.36-μm penetration depth, a new band is detected at 1017 cm^{-1} due to the Si—O—C asymmetric stretching modes [trace (A), Fig. 11]. Because the top latex layer was deposited when the bottom layer was already coalesced, MSMA molecules are detected in the interlayer region due to their diffusion into the bottom film, thus promoting interpenetration between the two latex layers.

Figure 12 shows ATR FTIR spectra recorded from the F–S interface of the bottom layer at various angles of incidence. Similar trends are found at the F–S interface, although their magnitude is different. It appears that the 1046 cm^{-1} band is stronger near the F–S interface, thus indicating that water evaporates out of latex after latex coalescence, and that only the outermost SDOSS molecules have the opportunity to form H-bonding with H_2O. The SDOSS molecules inside the film have less chances to associate with H_2O and acid groups, and therefore, the 1050 cm^{-1} band is detected at the deeper penetration depths. As we recall, the 1050 cm^{-1} band results from the S—O stretching modes of $SO_3^-Na^+$ groups that are likely not affected by the environment. As a matter of fact, the band intensities at 1046 and 1050 cm^{-1} are weaker at the F–A interface than at the F–S interface, indicating that more SDOSS molecules exude toward the F–S interface.

As we mentioned earlier, more SDOSS molecules are detected near the F–A interface in silicone modified latex films. Interestingly, an opposite behavior was found for SDOSS exudation in the non-silicone-modified latex films, where a higher content of SDOSS molecules was detected near the F–S interface. Let us recall the S—O and Si—O stretching regions recorded with TE polarization in Figure 10.

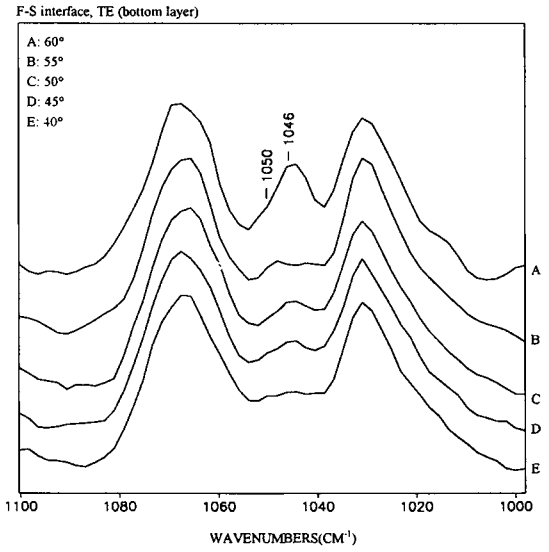

Figure 12 ATR FTIR spectra of S—O symmetric stretching vibrational modes of 50/50% Sty/*n*-BA composition containing 10% MSMA with various incident angles of IR light at F–S interface of bottom layer with TE polarization: (A) 60°; (B) 55°; (C) 50°; (D) 45°; (E) 40°.

Trace (A) shows that the 1046 and 1017 cm^{-1} bands, due to the S—O and Si—O stretching normal vibrations, respectively, are detectable with TE polarization. However, these bands are not detectable when the spectra are recorded with transverse magnetic (TM) polarizations [Fig. 13, trace (A)]. Because polarized ATR data allow us to establish orientation of the dipole moment changes with respect to laboratory axes, we see that the $SO_3^-Na^+$ hydrophilic end groups and Si—O groups in MSMA are preferentially parallel to the film interfacial surface.

Based on the results presented above, we can deduce how MSMA and SDOSS molecules act at the interfaces. As mentioned earlier, the distribution of the SDOSS and MSMA molecules is influenced by the bottom latex film properties in a double-layer latex film. This is reflected in the decreasing band intensity at 1046 cm^{-1} with the increasing depth of penetration near the F–A_{Top} interface in double-layer latex films. A schematic diagram of the molecular arrangements of the double-layered film is illustrated in Figure 14. It appears that there are no differences between the TE (Fig. 9) and TM (not shown) polarizations near the F–A_{Top} interface, and the SDOSS molecules have no preferential orientation. This is illustrated in Figure 14 (F–A_{Top} interface). In contrast, the 1046 cm^{-1} band is enhanced in the TE polarization (Fig. 10), and this band is not detectable in the TM polarization (Fig. 13), indicating that the hydrophilic $SO_3^-Na^+$ ends are preferentially parallel to the F–F interface. Since the 1017 cm^{-1} band is detected only in the TE polarization (Fig. 10), and not detected with TM polarization (Fig. 13), MSMA molecules are preferentially parallel to the film surface. They are shown in Figure 14, marked as the F–F interface. Similarly, there are no detectable differences between the TE (Fig. 12) and TM (not shown) polarizations near the F–S interface, indicating that the SDOSS molecules have a random orientation near the F–S interface shown in Figure 14 (marked as the F–S interface).

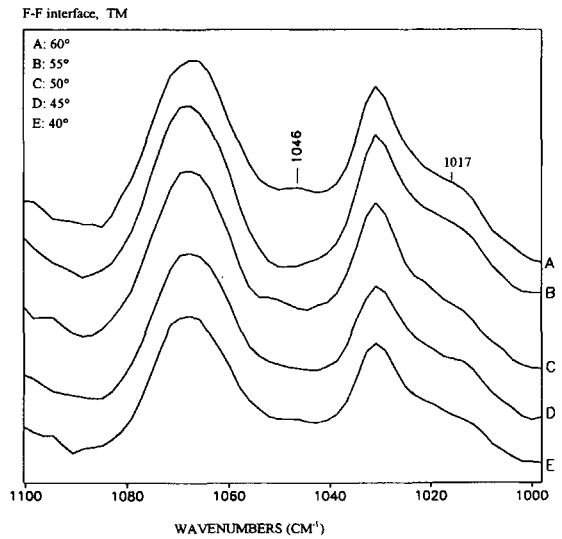

Figure 13 ATR FTIR spectra of S—O symmetric stretching vibrational modes of 50/50% Sty/*n*-BA composition containing 10% MSMA with various incident angles of IR light at F–S interface of top layer with TM polarization: (A) 60°; (B) 55°; (C) 50°; (D) 45°; (E) 40°.

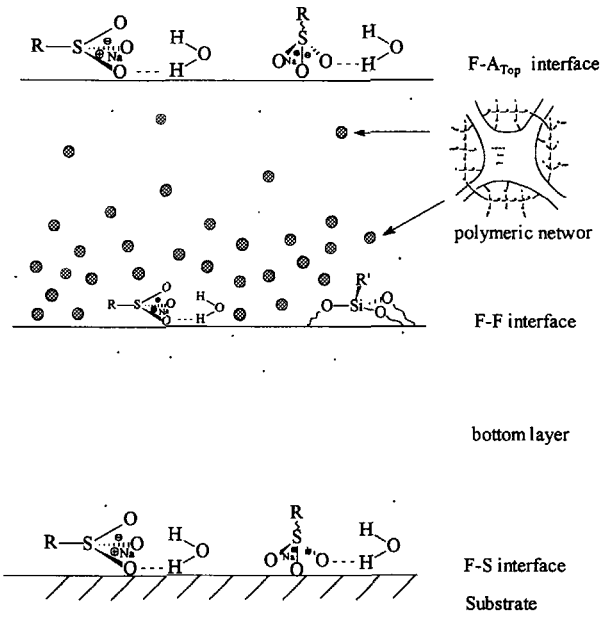

Figure 14 Schematic diagram of SDOSS and MSMA molecular arrangements.

In conclusion, let us reexamine Figure 1 and realize that if the IPN is formed, we would expect to see a uniform distribution of MSMA molecules across the film. However, the MSMA molecules are concentrated near the F–S interface, indicating that if the IPN were formed, it would be highly localized. Therefore, these results show that there is a significant gradient of properties across the film. As a matter of fact, these—as well as our previous studies[10–15,17]—indicate that the concept of IPN, or the phase separation within polymer networks forming polymeric films, is strongly affected by the film formation. Namely, there may be a significant difference in the network properties between the F–A and F–S interfaces.

CONCLUSIONS

In this study, SDOSS surfactant mobility in single- and double-layer silicone modified latex films were

examined using polarized ATR FTIR spectroscopy. Based on these studies, the orientation of SDOSS near the F–A_{Top}, F–F, and F–S interfaces was identified. Whereas SDOSS is detected near the F–A interface in the single-layer silicone-modified latex film, there is no SDOSS near the F–S interface due to its displacement by MSMA. In double-layer latex films, SDOSS is presented near the F–A_{Top} interface, and the hydrophilic $SO_3^-Na^+$ ends have no preferential orientation at this interface. However, hydrophilic $SO_3^-Na^+$ ends are preferentially parallel in the interfacial double-layer region. At the F–S interface, SDOSS molecules have no preferential orientation. Based on the spectroscopic data, a higher content of MSMA molecules is detected near the F–S interface. However, in the double-layer latex film, a higher content of MSMA is detected in the F–F interface and the MSMA molecules are preferentially parallel to the F–F interface.

REFERENCES

1. E. P. Plueddemann, *Prog. Org. Coat.*, **11,** 297 (1983).
2. G. L. Witucki, *J. Coat. Tech.*, **65**(822), 57 (1993).
3. M. W. Urban and K. W. Evanson, *Polym. Commun.*, **31,** 279 (1990).
4. J. B. Huang and M. W. Urban, *Appl. Spectrosc.*, **46**(11), 1666 (1992).
5. J. B. Huang and M. W. Urban, *Appl. Spectrosc.*, **47**(7), 973 (1993).
6. K. W. Evanson and M. W. Urban, *J. Appl. Polym. Sci.*, **42,** 2287 (1991).
7. K. W. Evanson, T. A. Thorstenson, and M. W. Urban, *J. Appl. Polym. Sci.*, **42,** 2297 (1991).
8. T. A. Thorstenson, K. W. Evanson, and M. W. Urban, *Polym. Mater. Sci. Eng.*, **64,** 195 (1991).
9. K. W. Evanson and M. W. Urban, *J. Appl. Polym. Sci.*, **42,** 2309 (1991).
10. T. A. Thorstenson and M. W. Urban, *J. Appl. Polym. Sci.*, **47,** 1381 (1993).
11. T. A. Thorstenson and M. W. Urban, *J. Appl. Polym. Sci.*, **47,** 1387 (1993).
12. T. A. Thorstenson, L. K. Tebelius, and M. W. Urban, *J. Appl. Polym. Sci.*, **49,** 103 (1993).
13. T. A. Thorstenson, L. K. Tebelius, and M. W. Urban, *J. Appl. Polym. Sci.*, **50,** 1207 (1993).
14. J. P. Kunkel and M. W. Urban, *J. Appl. Polym. Sci.*, **50,** 1217 (1993).
15. B.-J. Niu and M. W. Urban, *J. Appl. Polym. Sci.*, **56,** 377 (1995).
16. M. W. Urban, *Vibrational Spectroscopy of Molecules and Macromolecules on Surfaces,* Wiley-Interscience Publishers, New York, 1993, Chap. 8.
17. B.-J. Niu and M. W. Urban, to appear.

Received June 26, 1995
Accepted October 1, 1995